

## IMECE2008-66937-Draft

### LOCAL GEOMETRIC PROJECTION BASED NOISE REDUCTION FOR VIBRATION SIGNAL ANALYSIS IN ROLLING BEARINGS

**Ruqiang Yan**

Dept. of Mechanical & Industrial Engineering  
University of Massachusetts  
Amherst, MA 01003  
E-mail: ryan@ecs.umass.edu

**Robert X. Gao**

Dept. of Mechanical & Industrial Engineering  
University of Massachusetts  
Amherst, MA 01003  
E-mail: gao@ecs.umass.edu

**Kang B. Lee**

Manufacturing Metrology Division  
National Institute of Standards and Technology  
Gaithersburg, MD 20899  
Email: kang.lee@nist.gov

**Steven E. Fick**

Manufacturing Metrology Division  
National Institute of Standards and Technology  
Gaithersburg, MD 20899  
Email: steven.fick@nist.gov

#### ABSTRACT

*This paper presents a local geometric projection (LGP)-based noise reduction approach to vibration signal analysis in rolling bearings. LGP is a non-linear filtering technique that reconstructs one dimensional time series in a high-dimensional phase space using time-delayed coordinates based on the Takens embedding theorem. From the neighborhood of each point in the phase space, where a neighbor is defined as a local subspace of the whole phase space, the best subspace that the point will be orthogonally projected to is identified. Since the signal subspace is formed by the most significant eigen-directions of the neighborhood, while the less significant ones define the noise subspace, the noise can be reduced by converting the points onto the subspace spanned by those significant eigen-directions back to a new, one-dimensional time series.*

*The proposed approach is first evaluated using a chaotic system and an analytically formulated synthetic signal in terms of signal-to-noise ratio improvement. Then a case study on bearing vibration signal is carried out. The proposed technique is shown to be effective in reducing noise and enhancing extraction of weak, defect-related features from the signal, thus contributing to bearing condition monitoring and health diagnosis.*

#### I. INTRODUCTION

Machine condition monitoring and health diagnosis have been an active research area attracting increasing attention from the research community worldwide. Since the occurrence of failures in machine systems is generally accompanied by

change of its dynamic characteristics, vibration measurement has been routinely conducted for defect monitoring and diagnosis. Linear, weak nonlinear or strongly nonlinear behaviors have been observed in vibration signals, reflecting upon the various working conditions of the machines. It was found that non-linear chaotic vibrations were generated in gear systems [1], rolling bearings [2], or generator with a cracked rotor [3]. These observations indicate that non-linear dynamics provide a complementary approach to commonly employed techniques such as spectrum analysis or time-frequency-scale analysis for machine condition monitoring and health diagnosis.

Development of non-linear dynamics theory has introduced new quantities such as correlation dimension, multifractal spectrum, and Lyapunov exponent to interpret signals measured from physical systems where chaotic behaviors are identified. Over the past decade, application of these quantities has been increasingly explored. As an example, correlation dimension of bearing vibration signals were analyzed and three types of bearing faults were identified from their respective values [4]. The correlation dimension was also able to identify fatigue crack and broken tooth in a gearbox [5]. In another study, the multi-fractal spectrum has shown to be a viable tool for identifying defective machine components [6]. In [7] the Lyapunov exponent spectrum extracted from vibration signals was utilized to classify different bearing defects. These quantities, however, were found to be sensitive to the presence of noise [8]. Considering that the signal-to-noise ratio (SNR) of the measured data is low at the early stage of defect inception due to the relatively weak amplitude

induced by the defects and structural attenuation between the source of signal generation and the sensor location, it is important to develop noise reduction techniques to ensure effectiveness of non-linear measures for machine condition monitoring and health diagnosis.

For denoising vibration signals in which non-linear behavior is identified, traditional filters (e.g., low-pass filter and band-pass filter, etc.) may not work well, as they are only effective in conditions where the noise is confined within a known frequency range. Furthermore, the filters may induce distortion due to the fact that some of the frequency components that characterize the system dynamics can also be suppressed by simply applying these filters. Various studies have been conducted to overcome the difficulty of noise reduction involved in nonlinear behavior [9-14]. For example, a dynamical learning technique was combined with a least-square trajectory procedure to perform noise reduction [10]. A shadowing-based approach was proposed to treat nonlinear chaotic signal [11]. This approach was also integrated with statistical method to achieve comparable denoising results [12]. In another study, local constant fits were used to obtain denoised data in a reconstructed phase space [13]. Study in [14] developed a local geometric projection (LGP) technique for noise reduction in chaotic maps and flows. Among various approaches described above, the LGP has been investigated by researchers in terms of improving its effectiveness on noise reduction [15, 16], and successfully applied to various problems [17-19]. It was observed that in the analysis of heart rate variability, values of correlation dimension change after noise reduction [17]. When the LGP method was used for Chinese speech enhancement [18], better performance was shown as compared to two popular algorithms: the E-M and E-V methods. Moreover, weak harmonic signals from chaotic interference were reported to have been extracted using LGP-based noise reduction [19].

This paper investigates the utility of LGP for reducing noise contained in vibration signals measured on rolling bearings, with specific application in rolling bearings. The paper is organized as follows. Section II introduces the theoretical basis of the LGP algorithm, in which various parameters, such as dimension and delay time for reconstruction that affect the effectiveness of the noise reduction algorithm, are discussed. Simulation using a well-known chaotic system and an analytically formulated synthetic signal were conducted in section III to quantify the effect of signal-to-noise ratio improvement. In section IV, the LGP application to bearing vibration signals is experimentally investigated. Finally, conclusions are drawn in section V.

## II. LOCAL GEOMETRIC PROJECTION

Suppose a time series  $\{\bar{x}_1, \bar{x}_2, \dots, \bar{x}_N\}$  represents true observable quantities of a given dynamic system. Due to the existence of noise contamination, the measured time series  $\{x_1, x_2, \dots, x_N\}$  is expressed as:

$$x_n = \bar{x}_n + \eta_n \quad n=1,2,\dots,N \quad (1)$$

where  $\eta_n$  denotes the noise component. The ultimate goal of any noise reduction algorithm is to estimate the time series  $\{\bar{x}_1, \bar{x}_2, \dots, \bar{x}_N\}$  from the measured one  $\{x_1, x_2, \dots, x_N\}$  such that the following condition is satisfied:

$$\hat{x}_n \approx x_n - \delta x_n \quad n=1,2,\dots,N \quad (2)$$

where  $\hat{x}_n$  represents the estimation of  $\bar{x}_n$  and  $\delta x_n$  denotes the corrections. Combining Eq. (1) with Eq. (2) results in:

$$\hat{x}_n \approx \bar{x}_n + \eta_n - \delta x_n \quad n=1,2,\dots,N \quad (3)$$

Equation (3) indicates an idea noise reduction technique should make the term  $\eta_n - \delta x_n$  be equal or close to zero.

The LGP algorithm technique studied in this paper was developed from the view of a phase space perspective, and it does not require any prior information on the underlying dynamics of systems being investigated for its implementation [14]. This main idea of the technique is that in a multi-dimensional phase space reconstructed from the measured time series, the true observable quantities and the measurement noise can be decomposed into different local subspaces by orthogonal projection. Through rebuilding these local subspaces that are only occupied by those observable quantities, a new time series can be converted back with the measurement noise being removed. Four major steps: 1) phase space reconstruction, 2) neighborhood covering, 3) local subspace projection, and 4) new time series conversion, are involved in the whole process when implementing the algorithm. They are discussed in detail as follows.

## Phase Space Reconstruction

In practice, the actual phase space of a dynamic system can seldom be obtained. To solve this problem, the time-delayed coordinates approach based on the Takens embedding theorem [20] is applied to reconstruct the phase space from only one measured time series of the system. For the measured time series  $\{x(1), x(2), \dots, x(N)\}$ , a series of vectors  $X(i)$  in the reconstructed phase space is generated as:

$$\begin{cases} X(1) = \{x(1), x(1+\tau), \dots, x(1+(m-1)\tau)\} \\ \dots \\ X(i) = \{x(i), x(i+\tau), \dots, x(i+(m-1)\tau)\} \\ \dots \\ X(N-(m-1)\tau) = \{x(N-(m-1)\tau), x(N-(m-2)\tau), \dots, x(N)\} \end{cases} \quad (4)$$

where the parameters  $\tau$  and  $m$  are the time delay and the embedding dimension of the reconstructed phase space, respectively. According to the Takens theory [20], a sufficient condition for the embedding dimension was given as  $m \geq 2d + 1$ , where  $d$  is the fractal dimension of the analyzed system. Takens also assumed there are no constraints for the selection of time delay  $\tau$  if infinite number of noise-free data points can be obtained. However, since the measured time series only contains a finite number of data points that is contaminated by measurement noise, the time delay  $\tau$  needs to

be chosen appropriately so that the underlying dynamics in the reconstructed phase space and original system are equivalent in the topological sense. Furthermore, the time delay  $\tau$  can not be chosen to be too small, as it will make the reconstructed vectors not significantly differ from each other. On the other hand, if the time delay  $\tau$  is too large, the time-delay coordinates will be uncorrelated, and no useful information can be obtained from them to illustrate the underlying dynamics of the system. Various approaches have been developed to determine the parameters  $\tau$  and  $m$ , such as autocorrelation function [9] and mutual information [21] for time delay  $\tau$ , G-P algorithm [22] and False Nearest Neighbors (FNN) [23] for embedding dimension. These approaches assume the selection of the parameters  $\tau$  and  $m$  is independent. In the present study, the time delay and embedding dimension are determined at the same time using the C-C method based on the concept of embedding window [24].

### Neighborhood Covering

Subsequent to the phase space reconstruction, a reference point  $X_1^1$  is randomly chosen from all the points  $X(i)$  ( $i = 1, 2, \dots, N - (m-1)\tau$ ) as shown in Eq. (4). By finding its  $l$ -1 nearest neighbor points, a neighborhood is formed as:

$$U_1 = \{X_1^1, X_2^1, \dots, X_l^1\} \quad (5)$$

where  $l$  represents the number of points in the neighborhood, and it should be larger than the embedding dimension  $m$ .

With the same procedure, the next  $N_b - 1$  reference points  $X_1^h$  ( $h = 2, 3, \dots, N_b$ ) are selected and subsequently formulate their corresponding neighborhoods as

$$U_j = \{X_1^j, X_2^j, \dots, X_l^j\} \quad j = 2, 3, \dots, N_b \quad (6)$$

It should be noted that the selection of reference point  $X_1^h$  is subject to the condition  $X_1^h \notin U_k$  ( $k = 1, 2, \dots, N_b$ ) when  $h \neq k$ . All the  $N_b$  locally formulated neighborhoods work together to cover the entire phase space.

### Local Subspace Projection

For each formulated neighborhood, the sample average is calculated as:

$$a_k = \sum_{t=1}^l X_t^k / l \quad (7)$$

By defining the neighborhood radius as:

$$r_k = \max_{t=1, 2, \dots, l} \|a_k - X_t^k\| \quad X_t^k \in U_k \quad (8)$$

all the neighborhoods can be reordered as

$$M = \{(X_1^1, U_1), (X_1^2, U_2), \dots, (X_1^{N_b}, U_{N_b})\} \quad (9)$$

with increasing  $r_k$ . The covariance matrix  $C_k$  of the points in each neighborhood is then calculated as:

$$C_k = \frac{1}{l} \sum_{t=1}^l [X_t^k - a_k][X_t^k - a_k]^T \quad (10)$$

Performing singular value decomposition on the covariance matrix  $C_k$  leads to

$$C_k = A_k \Lambda_k A_k^T \quad (11)$$

where  $A_k$  is a  $m \times m$  matrix whose columns are orthonormal eigenvectors of the covariance matrix, and  $A_k A_k^T = I_m$ . The symbol  $\Lambda_k$  is a diagonal matrix whose diagonal elements  $\lambda_1 \geq \lambda_2 \geq \dots \geq \lambda_m$  are the eigenvalues of the covariance matrix. Research in [9] stated that in the  $m$  dimensional reconstructed phase space, the underlying dynamics of the system are only confined to a low dimensional subspace  $m_0$  ( $m_0 < m$ ). This means there exist  $m - m_0$  *null-spaces* in the reconstructed phase space. If any information can be found in these *null-spaces*, that must be caused by the noise. Therefore, by only projecting the points in the neighborhood into the  $m_0$  subspace, noise can be removed. The projection operator from  $m$  dimensional phase space to  $m_0$  dimensional subspace is technically achieved as:

$$P_k = B_k B_k^T \quad (12)$$

where  $B_k$  is the matrix whose columns are the first  $m_0$  eigenvectors in  $A_k$ , which correspond to the largest  $m_0$  eigenvalues of the covariance matrix  $C_k$ . All the points in the neighborhood  $U_k$  ( $k = 1, 2, \dots, N_b$ ) are replaced by the new adjusted points as

$$\hat{X}_t^k = a_k + P_k(X_t^k - a_k) \quad t = 1, 2, \dots, l \quad (13)$$

The local subspace projection is performed with the sequence shown in Eq. (9), as starting with small neighborhood radius ensures better estimate of underlying dynamics of the system within a local region of the reconstructed phase space [14]. Since each point  $\hat{X}_t^k$  has a corresponding one (denoted as a vector) in Eq. (4). The vectors originally generated in the reconstructed phase space shown in Eq. (4) are adjusted as  $\hat{X}(i)$  ( $i = 1, 2, \dots, N - (m-1)\tau$ ).

### New Time Series Conversion

From the adjusted vectors  $\hat{X}(i)$  ( $i = 1, 2, \dots, N - (m-1)\tau$ ), a new time series with noise being removed can be constructed. According to the statement in [14], the best new time series outputs the minimum error  $\varepsilon$  in the following equation:

$$\varepsilon = \min \left( \sum_{i=1}^{N-(m-1)\tau} \sum_{q=1}^m \left[ \hat{X}_q(i) - \hat{x}(i+(q-1)\tau) \right]^2 \right) \quad (14)$$

where  $\hat{X}_q(i)$  denotes the  $q$  element in the adjusted vector  $\hat{X}(i)$ . Accordingly, the new time series is obtained as [14]:

$$\hat{x}(i) = \begin{cases} \frac{1}{s} \sum_{q=1}^s \hat{X}_q(i-(q-1)\tau) & 1+(s-1)\tau \leq i \leq s\tau, s=1,2,\dots,m-1 \\ \frac{1}{m} \sum_{q=1}^m \hat{X}_q(i-(q-1)\tau) & 1+(m-1)\tau \leq i \leq N-(m-1)\tau \\ \frac{1}{s} \sum_{q=m-s+1}^m \hat{X}_q(i-(q-1)\tau) & 1+N-s\tau \leq i \leq N-(s-1)\tau, s=m-1,\dots,1 \end{cases} \quad (15)$$

Quantitative measures can be further extracted from this noise cleaned time series  $\{\hat{x}(1), \hat{x}(2), \dots, \hat{x}(N)\}$  to characterize the dynamic system being investigated.

### III. SIMULATION OF ALGORITHM

To quantitatively evaluate the LGP-based noise reduction algorithm, two simulation studies were carried out. The first study began with a time series generated from a well-known nonlinear dynamic system: the Lorenz system, and was contaminated by noise. The second study was a time series from an analytically formulated synthetic signal that describes a series of equally spaced impulsive vibrations added with different level of white noise.

#### Lorenz System

The Lorenz system is a typical nonlinear dynamic system, which is derived from simplified equations of convection rolls arising in the equations of the atmosphere [25], and is expressed as:

$$\begin{cases} \frac{dx}{dt} = \sigma(y-x) \\ \frac{dy}{dt} = \rho x - y - xz \\ \frac{dz}{dt} = -\beta z + xy \end{cases} \quad (16)$$

where  $\sigma$  is the Prandtl number,  $\rho$  is the Rayleigh number. When  $\sigma=10$ ,  $\rho=28$ , and  $\beta=8/3$ , the system exhibits chaotic behavior. Figure 1 illustrates the Lorenz signal in the  $x$  (vertical) direction, which expresses the convection intensity of the atmosphere. It should be noted that all the operations investigated here are applicable to the Lorenz signal in other two directions. Figure 2 illustrates the noise contaminated Lorenz signal in  $x$  direction, in which a 20 dB white noise is added. After the LGP-based noise reduction approach is applied to the signal, the result shown in Fig. 3 indicates that a 10.3 dB signal-to-noise ratio improvement (i.e. 30.3 dB vs. 20. dB) is achieved.

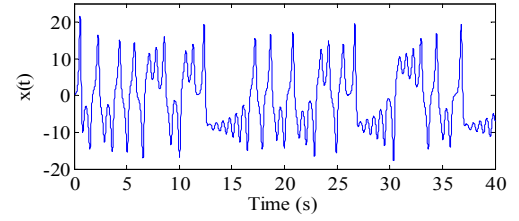


Fig. 1. Lorenz signal in x direction (noise free)

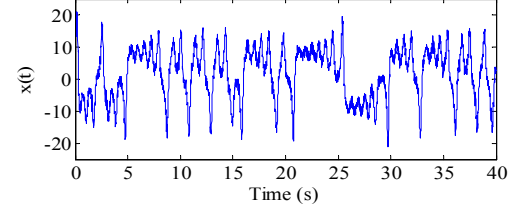


Fig. 2. Lorenz signal with additive white noise (SNR=20 dB)

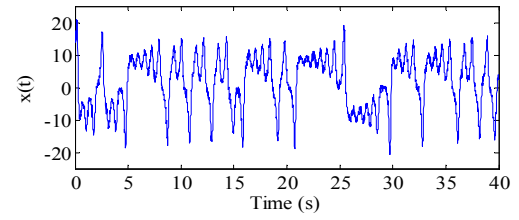


Fig. 3. Lorenz signal after noise reduction (SNR=30.3 dB)

Further study has been conducted on the Lorenz system with different level of white noise being added. As can be seen from the results listed in Table I, the LGP-based noise reduction approach was able to effectively improve the signal-to-noise ratio of the Lorenz signal.

Table I. LGP noise reduction results under different SNRs

SNR		
Before LGP (dB)	After LGP (dB)	Improvement (dB)
1	5.1	4.1
3	7.2	4.2
6	11.4	5.4
10	15.6	5.6
15	24.6	9.6
20	30.3	10.3

#### Synthetic Signal

To quantitatively evaluate the performance of the presented LGP approach for denoising vibration signals measured from a rolling bearing that contains defect-related information and noise contamination, a synthetic signal was formulated. Generally, vibration signals from a bearing may include the following constituent components: 1) vibration caused by bearing unbalance with a characteristic frequency of  $f_u$ , which is equal to the bearing rotational speed and occurs when the gravitational center of the bearing does not coincide with its rotational center; 2) vibration caused by bearing misalignment at frequency  $f_m$ , which is equal to twice the shaft speed and

occurs when the two raceways of the bearing (inner and outer) fall out of the same plane, resulting in a raceway axis that is no longer parallel to the axis of the rotating shaft; 3) vibration due to rolling elements periodically passing over a fixed reference position on the outer raceway, at the frequency  $f_{BPFO}$ , and, 4) structure-borne vibration attributed by other components, which is broad-band and can be modeled as white noise.

When a localized structural defect occurs on the surface of the bearing raceways (inner or outer), a series of impacts will be generated every time the rolling elements interact with the defects, subsequently exciting the bearing system. Such forced vibration is represented by high frequency resonances that are amplitude-modulated at the repetition frequency of the impacts. For numerical simulation, defect-induced resonant vibration and structure-borne vibration are considered in the synthetic signal, as other vibration components can be filtered out through signal pre-processing. Defect-induced resonant vibration is simulated as a periodic Gaussian pulse signal as shown in Fig. 4. The pulse repetition frequency is 50 Hz, the sampling rate is 20 kHz, and pulse train length is 200 ms.

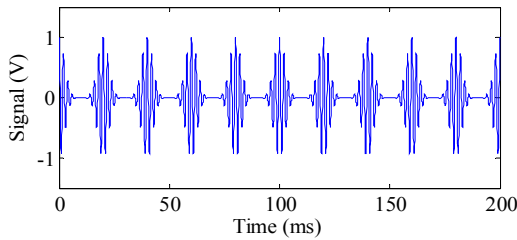


Fig. 4. Simulated defect-induced resonant vibrations

Structure-borne vibration is simulated as white noise. Figure 5 illustrates the synthetic signal formulated in this study, where the signal-to-noise ratio is 4 dB

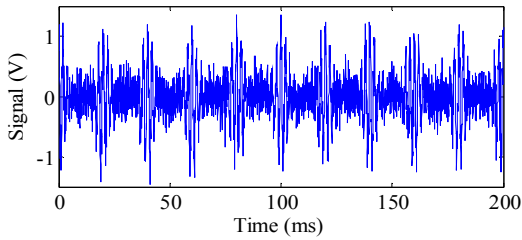


Fig. 5. The synthetic signal before noise reduction

After the LGP algorithm was applied to denoising the synthetic signal, the Gaussian pulses could be clearly identified, as shown in Fig. 6. The signal-to-noise ratio was improved to reach 10 dB.

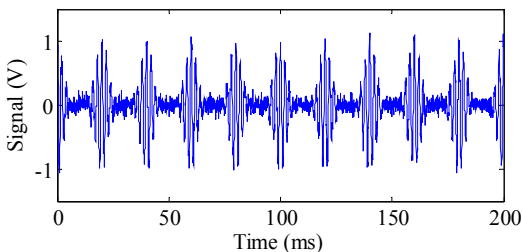


Fig. 6. The synthetic signal after noise reduction

#### IV. EXPERIMENTAL VERIFICATION

A case study has then been conducted on a pair of rolling element bearings (type 6205) to experimentally evaluate the effectiveness of the LGP-based noise reduction technique. One bearing is without any defect, and the other has a 0.1 mm-wide groove across its outer raceway. Vibration signals were measured on the two bearings under 1,440 rpm with a sampling frequency at 12,800 Hz. Figure 7 illustrates the waveforms of the measured signals.

The LGP algorithm was applied to the two vibration signals, respectively. As shown in Fig. 8b, a clearer pattern is seen than that show in Fig. 7b. The denoised signals can be further processed for defect identification. In this study, the multi-fractal spectrum  $h \sim D(h)$  (see details in [7]) of each signal is calculated. The width of the multi-fractal spectrum ( $\Delta h$ ), which is defined as  $\Delta h = h_{max} - h_{min}$ , with  $D(h_{max}) = D(h_{min}) = 0$ , and depicts the degree of singularity distribution of a signal is extracted as a measure for characterizing the vibration signals under different conditions.

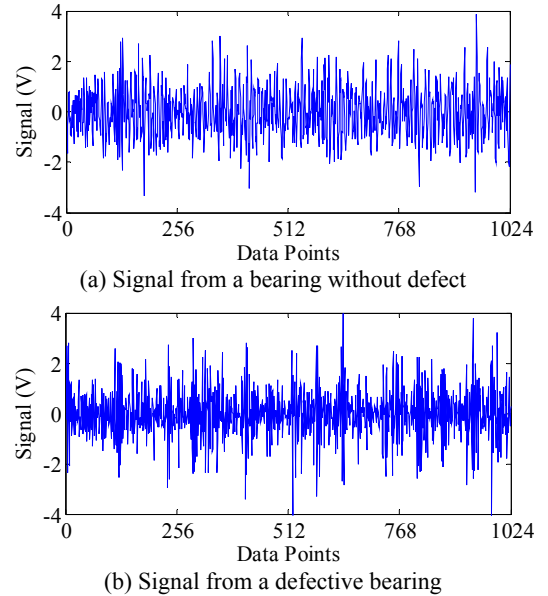
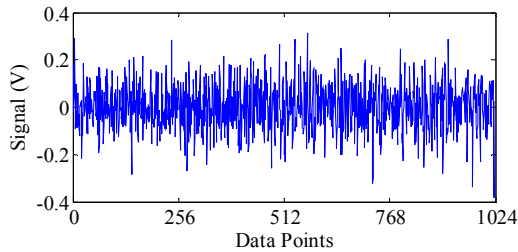
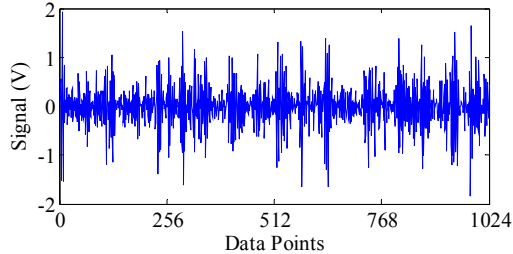


Fig. 7. Vibration signals measured from the test bearings before noise reduction

For purpose of comparison, Figures 9 and 10 illustrate the multi-fractal spectrum for both bearings before and after noise reduction, respectively. It can be seen that after LGP-denoising, the multi-fractal spectrum of the defective bearing becomes wider than that of the healthy bearing. This can be explained by the fact that the vibration signal from a defective bearing contain more frequency components (due to defect-induced vibrations), leading to a lower regularity of the signal and subsequently a wider singularity distribution. Furthermore, the difference of the width of the multi-fractal spectrum between the healthy bearing and defective bearing after noise reduction is larger than that before noise reduction (18% vs. 7.8%), as listed in Table II. This indicates the effectiveness of the LGP-based noise reduction in terms of bearing defect identification.



(a) Signal from a bearing without defect



(b) Signal from a defective bearing

Fig. 8. Vibration signals measured from the test bearings after noise reduction

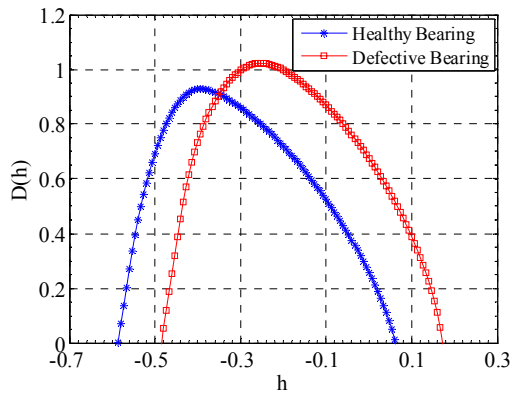


Fig. 9. Multi-fractal spectra of the bearing vibration signals before noise reduction

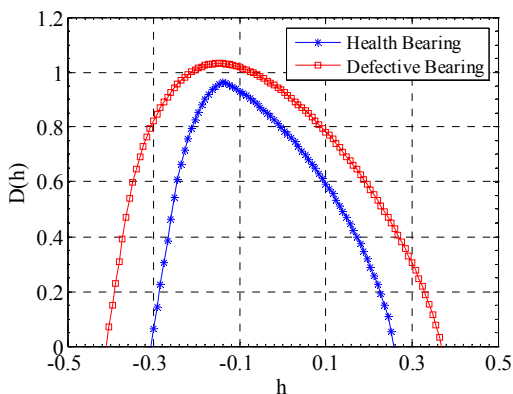


Fig. 10. Multi-fractal spectra of the bearing vibration signals after noise reduction

Table II. Multi-fractal spectrum parameters for test bearings

Bearing	$\Delta h$		
	Healthy	0.634	0.582
Defective	0.683	0.687	

## V. CONCLUSION

A local geometric projection based technique has been investigated with the goal to improve signal-to-noise ratio in dynamical signal decomposition and feature extraction. Different levels of white noise were added to a Lorenz signal to investigate the effectiveness of the presented noise reduction technique. As a measure for the noise reduction performance, the difference between the post-denoised and pre-denoised SNR of the Lorenz signal is calculated, and the results indicates the LGP-based technique is robust for denoising signals where nonlinear behavior exists. Subsequent studies on both simulated and experimental bearing vibration signals further demonstrated LGP as a viable signal processing tool for machine condition monitoring and health diagnosis.

## ACKNOWLEDGMENTS

This work was supported by the Advanced Manufacturing Systems Program at the National Institute of Standards and Technology (NIST).

\*\* This publication was prepared by United States Government employees as part of official duties and by guest researchers supported by federal funds. Therefore, this is a work of the U.S. Government and not subject to copyright.

## REFERENCES

- [1] Comparin, R.J. and Singh, R., 1990, "An Analytical Study of Automotive Neutral Gear Rattle", *Journal of Mechanical Design*, 112, pp. 237-245.
- [2] Ghafari, S.H., Golnaraghi, F., and Ismail F., 2007, "Effect of Localized Faults on Chaotic Vibration of Rolling Element Bearings", *Nonlinear Dynamics*, DOI 10.1007/s111071-007-9314-2.
- [3] Muller, P.C., Bajkowski, J., and Doffker, D., 1994, "Chaotic Motions and Fault Detection in a Cracked Rotor", *Nonlinear Dynamics*, 5, pp. 233-254.
- [4] Logan, D. and Mathew, J., 1996, "Using the Correlation Dimension for Vibration Fault Diagnosis of Rolling Element Bearing: Basic concepts", *Mechanical Systems and Signal Processing*, 10, pp. 241-250.
- [5] Jiang, J.D., Chen, J., and Qu, L.S., 1999, "The Application of Correlation Dimension in Gearbox Condition Monitoring", *Journal of Sound and Vibration*, 223(4), pp. 529-541.
- [6] Tao, X., Du, B., and Xu, Y., 2007, "Bearing Fault Diagnosis Based on GMM Model Using Lyapunov Exponent Spectrum", *Proceedings of 33<sup>rd</sup> Annual Conference of the Industrial Electronics Society*, Nov. 5-8, pp. 2666-2671.
- [7] Yan, R. and Gao, R., "Wavelet-Based Multi-fractal Spectrum for Machine Defect Identification", *ASME Conference on International Mechanical Engineering Congress and Exposition*, Paper No. 41984, Seattle, WA, November 11-15, 2007.
- [8] Kostelich, E. J. and Schreiber, T., 1993, "Noise Reduction in Chaotic Time Series Data: A Survey of Common Methods", *Physical Review E*, 48(3), September, pp. 1752-1763.

- [9] Kantz, H. and Schreiber T., 1997, *Nonlinear Time Series Analysis*, Cambridge University Press, UK.
- [10] Kostelich, E. J. and Yorke J.A., 1988, "Noise Reduction in Dynamics Systems", *Physical Review A*, 38(3), pp. 1649-1952.
- [11] Hammel, S.M., 1990, "A Noise Reduction Method for Chaotic System", *Physics Letter A*, 148(8,9), pp. 421-428.
- [12] Farmer, J.D. and Sidorowich, J.J., 1991, "Optimal Shadowing and Noise Reduction", *Physica D*, 47(30), pp. 373-392.
- [13] Schreiber, T., 1993, "Extremely Simple Nonlinear Noise-Reduction Method", *Physical Review E*, 47(4), April, pp. 2401-2404.
- [14] Cawley, R. and Hsu, G. H., 1992, "Local Geometric Projection Method for Noise Reduction in Chaotic Maps and Flows", *Physical Review A*, 46(6), September, pp. 3057-3082.
- [15] Urbanowicz, K. and Holyst, J. A., 2004, "Noise Reduction in Chaotic Time Series by a Local Projection with Nonlinear Constraints", *Acta Physica Polonica B*, 35(9), pp. 2175-2197.
- [16] Leontitsis, A., Bountis, T., and Pagge, J., 2004, "An Adaptive Way for Improving Noise Reduction Using Local Geometric Projection", *Chaos*, 14(1), March, pp. 106-110.
- [17] Signorini, M. G., Marchetti, F., and Cerutti, S., 2001, "Applying Nonlinear Noise Reduction in the Analysis of Heart Rate Variability", *IEEE Engineering in Medicine and Biology Magazine*, 20(2), March/April, pp. 59-68.
- [18] Sun, J., Zheng, N., and Wang, X., 2007, "Enhancement of Chinese Speech Based on Nonlinear Dynamics", *Signal Processing*, 87, pp. 2431-2445.
- [19] Wang, F., Wang, Z., and Gao J., 2002, "Extracting Weak Harmonic Signals From Strong Chaotic Interference", *Circuits Systems Signal Processing*, 21(4), pp. 427-448.
- [20] Takens, F. 1981, "Detecting Strange Attractors in Turbulence", *Dynamical Systems and Turbulence*, Lecture Notes in Mathematics, Rand, D. A. and Young, L.S (Eds.), Springer-Verlag, Berlin, pp. 366-381.
- [21] Fraser, A.M. and Swinney H.L., 1986, "Independent Coordinates for Strange Attractors from mutual information", *Physical Review A*, 33, pp. 1134-1140.
- [22] Grassberger, P. and Procaccia, I., 1983, "Measuring the Strangeness of Strange Attractors", *Physica D*, 9, pp.189-208.
- [23] Kennel, M.B., Brown, R., and Abarbanel, H.D., 1992, "Determining Embedding Dimension for Phase-Space Reconstruction Using a Geometrical Construction", *Physical Review A*, 45(6), pp.3403-3411.
- [24] Kim, H.S., Eykholt, R., and Salas, J.D., 1999, "Nonlinear Dynamics, Delay Times and Embedding Windows", *Physica D*, 127, pp. 48-60.
- [25] Lorenz, E. N., 1963, "Deterministic Nonperiodic Flow", *Journal of the Atmospheric Sciences*, 20, pp.130-141.